Vol. 41, No. 3 (2019) 311-320, DOI: 10.24874/ti.2019.41.03.01

Tribology in Industry

www.tribology.rs

RESEARCH

Fundamental Study on No-lubricating Friction Characteristics Due to Anisotropy of Surface Properties Applied to Differential Gear

Y. Ebisuno[a], Y. Sato[b], M. Fukumoto[b]

[a]*Research and Development Division, Musashi Seimitsu Industry Co., Ltd, Japan,*
[b]*Department of Mechanical Engineering, Toyohashi University of Technology, Japan.*

Keywords:

Friction
Surface roughness
Anisotropic roughness
Crease direction
No lubrication

Corresponding author:

Y. Ebisuno
Research and Development Division,
Musashi Seimitsu Industry Co., Ltd,
Japan.
E-mail: yoshinobu_ebisuno@musashi.co.jp

A B S T R A C T

The solid frictional characteristics of surface roughness in combination with anisotropy were systematically investigated through linear reciprocating sliding tests on planar surfaces with no lubrication. Four types of test pieces with anisotropy and varying amounts of surface roughness controlled by polishing were prepared. For test pieces #800 and #3000, their friction coefficients did not change significantly based on anisotropic combination conditions and remained relatively constant at 0.35. In contrast, for test pieces #80 and #150, their friction coefficients changed significantly based on anisotropic combination conditions. Their friction coefficients were approximately 0.45 when their crease directions were parallel and sliding directions were orthogonal, approximately 0.3 when their crease directions and sliding directions were both parallel, and approximately 0.15 when their crease directions were orthogonal and sliding direction were parallel. Therefore, the anisotropic combination conditions in which test pieces #80 and #150 had orthogonal crease directions and parallel sliding directions yielded the smallest friction coefficient.

1. INTRODUCTION

In recent years, improving the fuel economy of vehicles has become a major social issue from the perspective of protection of the global environment. The proportion of friction loss in fuel consumption is particularly high. Therefore, realizing the reduction of friction loss has become an important technical issue [1,2]. In the differential gear automobile component, which is one of the main products manufactured by the organization with which one of the authors is affiliated, the pinion gear and the shaft that supports it work under heavy loads at low velocity, subjecting them to severe sliding conditions as a result of solid materials contacting each other. In the worst-case scenario, seizure may occur due to severe contact conditions the same as no lubrication. Although measures incorporating optimization of surface conditions are being investigated to remedy such issues, such methods are still based on experience and

are in the trial-and-error stage of development. Solid design guidelines for appropriate surface properties to achieve friction loss have yet to be established. Accordingly, as a first step, we aimed to acquire knowledge regarding friction between solid materials.

In previous studies on the frictional characteristics of surfaces without lubrication, the following studies have been reported. Gachot et al. described about the surface texturing that has been extensively studied in recent years as follows [3]. As far as dry contacts are concerned, fewer publications compared to lubricated contacts exist dealing with benefits of surface texturing. And, no proper optimization interms of the geometry can be deduced from the literature. Ivkovic et al. investigated the relationship between the static friction coefficient and the surface roughness by various processing, and showed that the larger the surface roughness, the larger the coefficient of static friction [4]. Sedlaček et al. Investigated the relationship between the friction coefficient and the surface roughness parameter by various processes. As a result, it was shown that high arithmetic mean roughness Ra induced that the friction coefficient was low in the samples of grinding and polishing [5,6]. Miyagawa investigated the relationship between the friction coefficient and the anisotropic roughness caused by the processing of surface [7]. As a result, it was shown that the plowing resistance was increased with the increase of the roughness, and that the friction in the perpendicular to the crease direction was equal to or greater than that in the parallel direction. Menezes et al. also investigated the relationship between the friction coefficient and the surface roughness parameter, and the relationship between the friction coefficient and the anisotropic roughness caused by the processing of the surface [8,9]. As a result, it was shown that the coefficient of friction does not change so much with the arithmetic mean roughness Ra, and the friction was greater when sliding parallel to the processing direction compared to the perpendicular direction.

Thus, there is less literature on friction under no lubrication, and each research may show different results, and the relationship between the surface roughness and the friction coefficient under no lubrication is still not clear. Therefore, more research reports on friction without lubrication are needed. According to the literature, sufficient investigation has not been performed on test pieces with planar contact surfaces in combination with anisotropic surface roughness created by creases.

Accordingly, in this study, to acquire a basic understanding of the simplified phenomena of contact and sliding between solid materials, test pieces with various anisotropic surface roughness characteristics were prepared. Through linear reciprocating sliding tests with planar contact between the test pieces with no lubrication, a systematic investigation of the solid frictional characteristics of different combinations of surface roughness and anisotropy was conducted.

2. TEST METHODS

2.1 Test conditions

Figure 1 presents a schematic diagram of the test method and test pieces. The test method set linear reciprocating sliding tests with planar contact. The test device utilized was the HEIDON Type14FW, manufactured by Shinto Scientific Co. Ltd. For test conditions, the load was set to a constant 0.98 N. The sliding velocities were set in the range of 1–100 mm/s reference the pinion gear and shaft and the sliding distance was set to 50 mm. To provide a consistent surrounding atmosphere, the friction tests were conducted at a room temperature of 25±1 °C and relative humidity of 50±5 %. Furthermore, because there may be variations in the initial contact between solid materials, a running-in operation was conducted as a preliminary test.

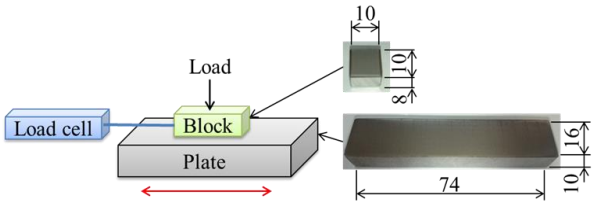

Fig. 1. Schematic diagram of test method and test pieces.

2.2 Test materials

S45C(252HV) steel was utilized as a test material. Material chemical compositions are listed in Table 1. Test piece blocks (10 mm (length)×10 mm (width)×8 mm (height) with a 0.5 mm×45° edge chamfer) and plates (74 mm

(length)×16 mm (width)×10 mm (height)) were hand polished on their contact surfaces by utilizing emery paper to impart anisotropic roughness in one direction. Four different test pieces with anisotropy and varying levels of surface roughness were prepared utilizing emery paper with different grain sizes. The test pieces were subjected to ultrasonic cleaning with acetone and dried with pressurized air.

Table 1. Material chemical compositions (%).

C	Si	Mn	P	S	Cu	Ni	Cr	Fe
0.44	0.21	0.72	0.12	0.15	0.01	0.01	0.18	balance

For each grain size (d50:median size) of the emery paper, the average values of the root-mean-squared height of the initial surface of the polished block and plate test pieces (Sq), skewness (Ssk), and kurtosis (Sku) are listed in Table 2. The error ranges for surface roughness (Sq) are presented in Fig. 2 and images of the initial surface morphologies of each of the test pieces are presented in Fig. 3. The surfaces of the test pieces were observed before and after the tests by a scanning-type white-light interferometric microscope.

Table 2. Average values of initial surface roughness.

Grain size (d50 [μm])	Test piece	surface roughness		
		Sq	Ssk	Sku
#80 (198)	Block	1.374	-0.580	3.815
	Plate	0.994	-0.881	5.324
#150 (99.0)	Block	0.485	-0.543	4.088
	Plate	0.449	-0.748	4.338
#800 (21.8)	Block	0.060	-0.349	3.783
	Plate	0.038	-0.570	5.361
#3000 (5.7)	Block	0.014	-0.325	3.311
	Plate	0.012	-0.480	4.791

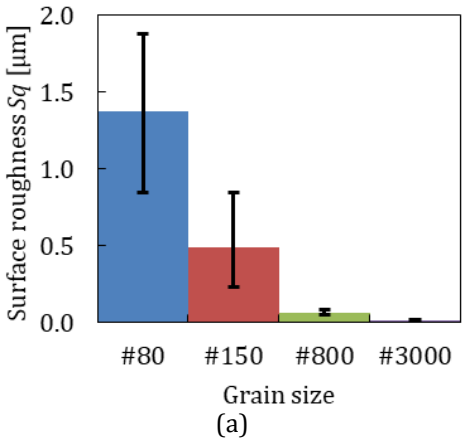

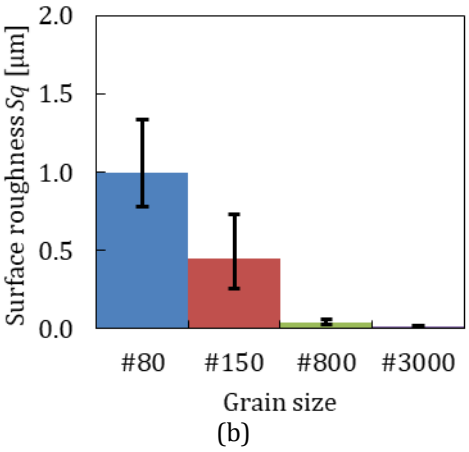

Fig. 2. Error ranges for surface roughness (Sq). (a) Block, (b) Plate.

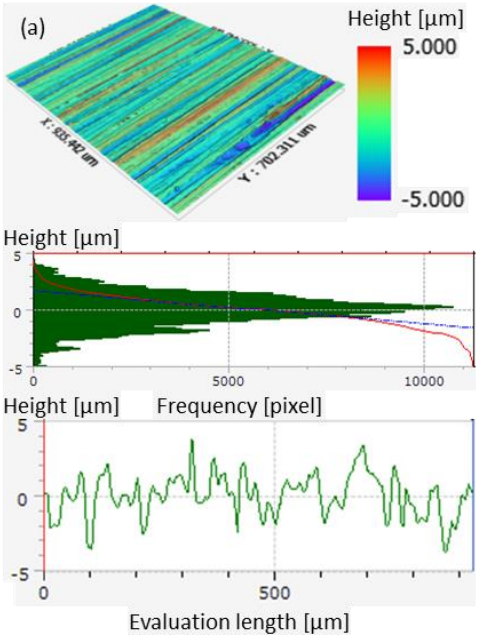

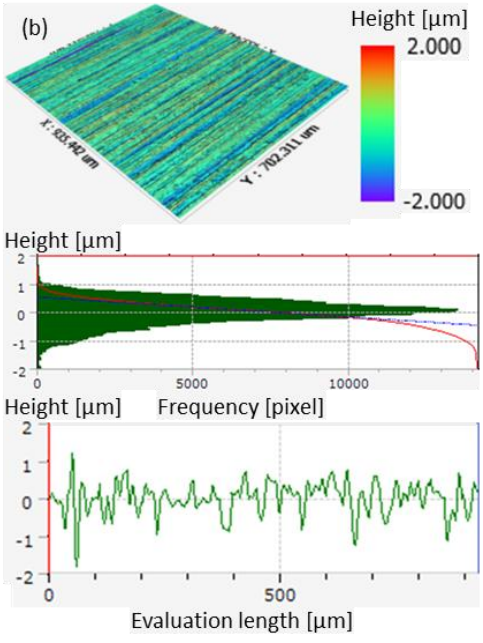

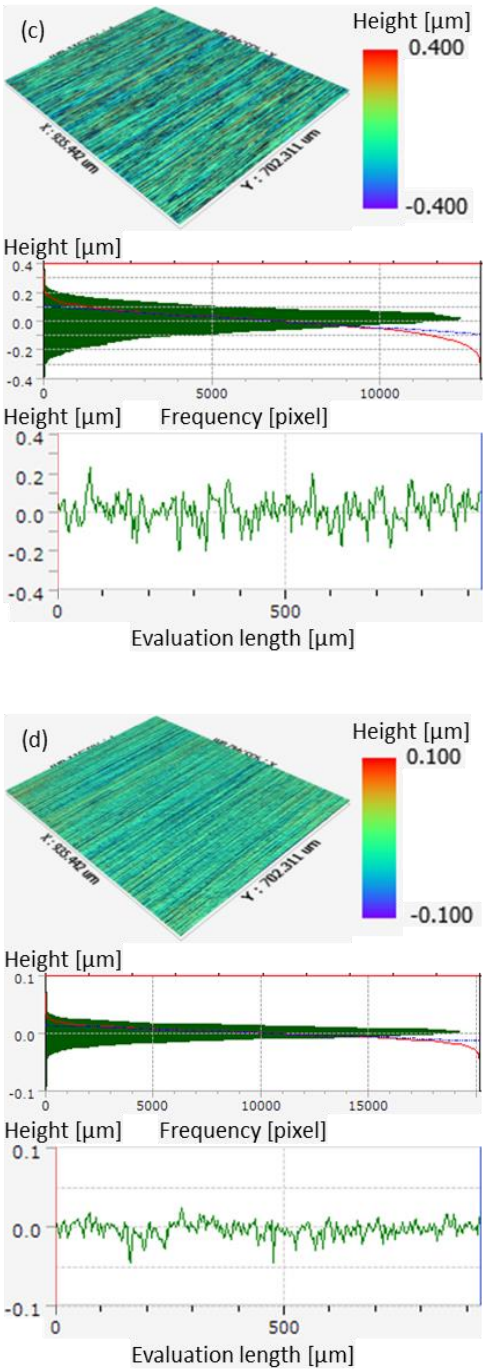

Fig. 3. Images of initial surface morphology of each test piece. Test piece (a) #80, (b) #150, (c) #800, (d) #3000.

2.3 Friction tests

Friction tests were conducted utilizing test pieces with consistent roughness under three different combinations of surface roughness crease direction and sliding direction such that the directions were either parallel or orthogonal to each other. Hereafter, these combinations of conditions are referred to as anisotropic combination conditions.

Figure 4 presents the three different anisotropic combination conditions. Under condition ①, the crease directions on the block and plate surfaces are parallel and the crease direction on the plate is parallel to the sliding direction. Under condition ②, the crease directions on the block and plate surfaces are parallel and the crease direction on the plate is orthogonal to the sliding direction. Under condition ③, the crease directions on the block and plate surfaces are orthogonal and the crease direction on the plate is parallel to the sliding direction.

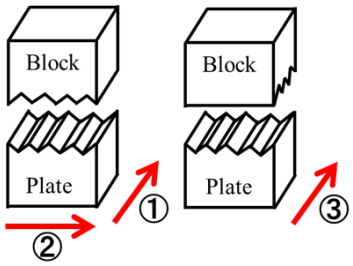

Fig. 4. Combination of crease direction and sliding direction. Arrows denote sliding directions.

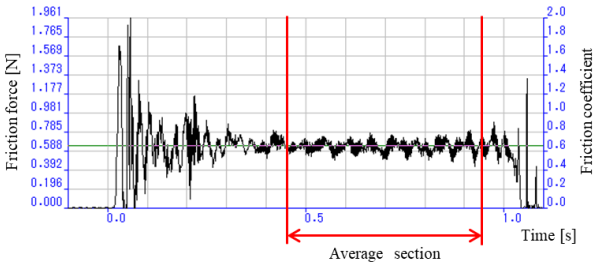

Fig. 5. Example average friction coefficient.

In our actual tests, after conducting the running-in operation, which will be described later, a test method in which the sliding velocity was gradually increased was adopted. For each sliding velocity, excluding the initial friction zone at rest, the average friction coefficient after the friction behavior stabilized was recorded as the friction coefficient for that condition. Figure 5 presents the method of capturing the average friction coefficient. Furthermore, for each type of surface roughness and anisotropic combination condition, the tests were conducted three times with new test pieces.

3. TEST RESULTS AND DISCUSSION

3.1 Changes in friction coefficient caused by running-in operation

In our test method, because wear can affect friction coefficients, the tests were repeated with

the same test piece by increasing the sliding velocity from 1 to 100 mm/s to investigate the change in friction coefficient. The test for the test piece and anisotropic combination condition for which the surface roughness changed the most (i.e., test piece #80 under anisotropic combination condition ②) was repeated three times without performing the running-in operation.

The results of these tests are presented in Fig. 6. Although the friction coefficient was slightly lower in the first test, from the second run onward, the results show a nearly constant friction coefficient. Based on these results, because the effect of wear on the friction coefficient was relatively small, the difference in values between the first and second runs can be attributed to the effects of initial conditioning (contact alignment) on the first run. After performing the running-in operation to exclude the effects of initial conditioning, factors related to the sliding velocity and reciprocation count were investigated.

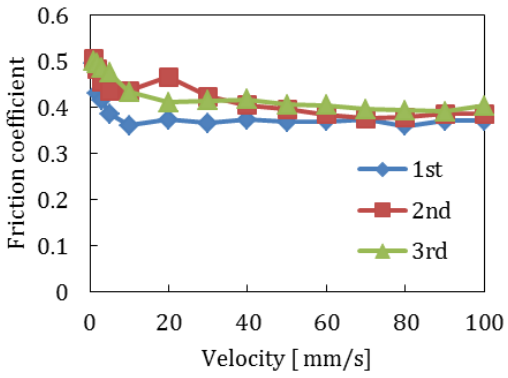

Fig. 6. Friction coefficient change over repeated trials under anisotropic combination condition ② for test piece #80 (1st-3rd denote trial numbers).

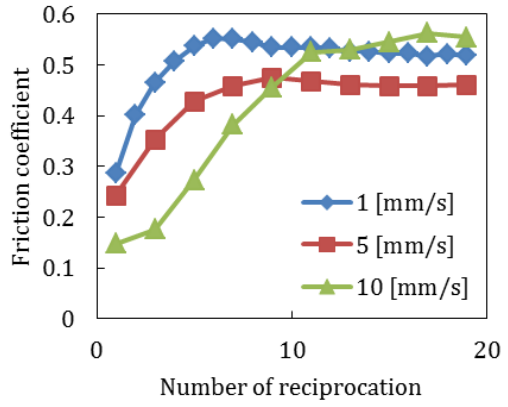

Fig. 7. Friction coefficient change with number of reciprocations under anisotropic combination condition ② for each sliding velocity.

Figure 7 presents the friction coefficient change with reciprocation count under anisotropic combination condition ② for test piece #80 with sliding velocities of 1, 5, and 10 mm/s. For all sliding velocities, we found that as the reciprocation count increased, the friction coefficient stabilized. Additionally, with an increase in sliding velocity, the reciprocation count at which the friction coefficient stabilized also increased. Based on these results, to avoid the effects of initial conditioning (contact alignment), the running-in operation was performed prior to all other experiments with a sliding velocity of 1 mm/s and reciprocation count of 10.

3.2 Friction coefficient changes caused by polishing grain size and anisotropic surface roughness

For each of the test pieces created with different polishing grain sizes, we performed friction tests under each of the anisotropic combination conditions to investigate the changes in friction coefficient with sliding velocity. Figure 8 presents a summary of the results for 12 different conditions. For all conditions, we confirmed that as the sliding velocity increased, the friction coefficient gradually decreased and converged to a constant value. Based on the results shown in Fig. 8, the following trends were identified regarding polishing grain size.

First, for test piece #80, under anisotropic combination condition ①, the friction coefficient changed significantly within the range of 0.2~0.5 with increasing sliding velocity. Under anisotropic combination condition ②, the scattering and change in the friction coefficient was smaller, but the final value was relatively high, falling in the range of 0.4~0.5. Under anisotropic combination condition ③, some scattering in the friction coefficient was observed, but the final value was low, falling in the range of 0.1~0.3.

Next, for test piece #150, under anisotropic combination condition ①, the friction coefficient showed a trend similar to that for test piece #80. Under anisotropic combination condition ②, compared to test piece #80, although the coefficient scattering was slightly larger, the value was similarly high, falling in the range of 0.35~0.55.

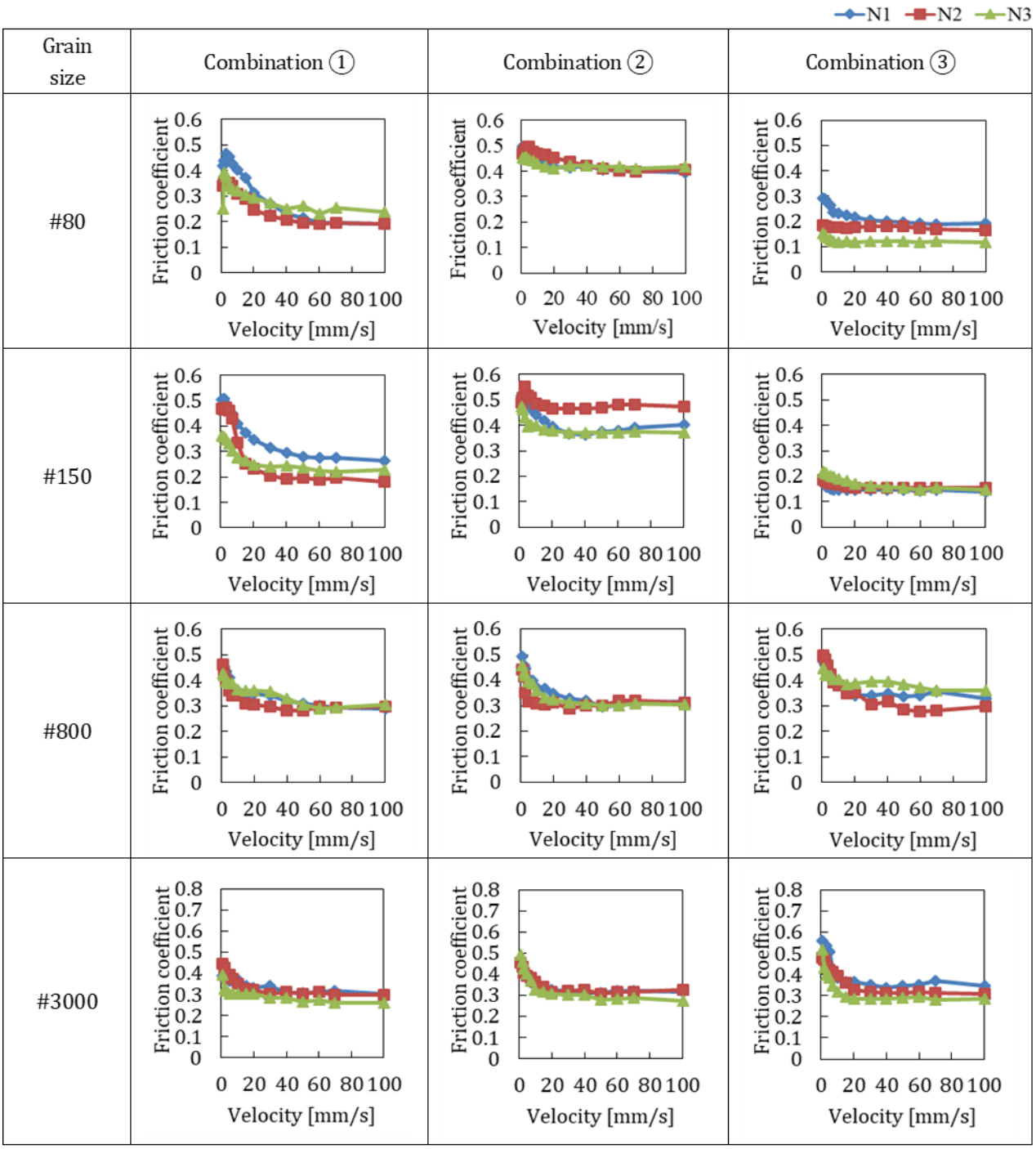

Fig. 8. Friction coefficient change with sliding velocity for each combination anisotropic combination condition for all test pieces (N1–N3 denote experimental iterations).

Under anisotropic combination condition ③, compared to test piece #80, the scattering and change in the friction coefficient with sliding velocity was smaller and the final value was lower, falling in the range of 0.15~0.2.

In contrast, for test pieces #800 and #3000, under all the anisotropic combination conditions, the friction coefficient converged within the range of 0.2~0.5.

3.3 Effects of surface roughness on friction coefficient

Because the main purpose of this study was to acquire knowledge regarding surface conditions to achieve lower friction loss, a relationship between surface roughness and the friction coefficient was derived based on the results above.

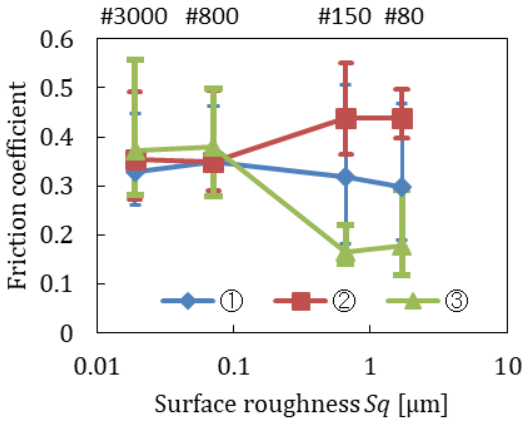

Fig. 9. Relationship between surface roughness (Sq) and average friction coefficient.

Figure 9 presents a summary of the average friction coefficients over the entire sliding velocity range, as well as the scattering of the friction coefficient with changes in sliding velocity, corresponding to the synthetic roughness values calculated based on the root-mean-squared height of the initial surface (Sq) under each of the anisotropic combination conditions. As shown in Fig. 9, for test pieces #800 and #3000, while the friction coefficient was constant at approximately 0.35, regardless of the anisotropic combination conditions, for test pieces #80 and #150, the friction coefficient changed significantly depending on the anisotropic combination conditions. While the friction coefficient was approximately 0.3 under anisotropic combination condition ①, regardless of the root-mean-squared height, it was relatively high at approximately 0.45 under anisotropic combination condition ②. In contrast, the value was relatively low at approximately 0.15 under anisotropic combination condition ③.

3.4 Discussion of the effects of the contact conditions of solid materials on friction coefficient and wear morphology

As mentioned above, because the contact conditions between solid materials strongly affect the changes in friction coefficient under different surface roughness and anisotropic combination conditions, the contact between solid materials and their wear morphologies were observed in detail by utilizing a scanning-type white-light interferometric microscope.

Figure 10 presents example images of the surface and cross-section profiles of test pieces #800 and #3000 after the friction tests. For both types of surface roughness, the wear morphology was similar under all conditions and a 100~200-μm width of linear wear marks was observed. Furthermore, because adhesion and the accumulation of wear powder was confirmed near the wear marks, we concluded that the wear morphology could be attributed to abrasive wear. Because the surface roughness of test pieces #800 and #3000 was relatively low, it is likely that the effects of anisotropic combination conditions on the contact conditions were smaller, causing the friction coefficient to converge to a similar value in both cases.

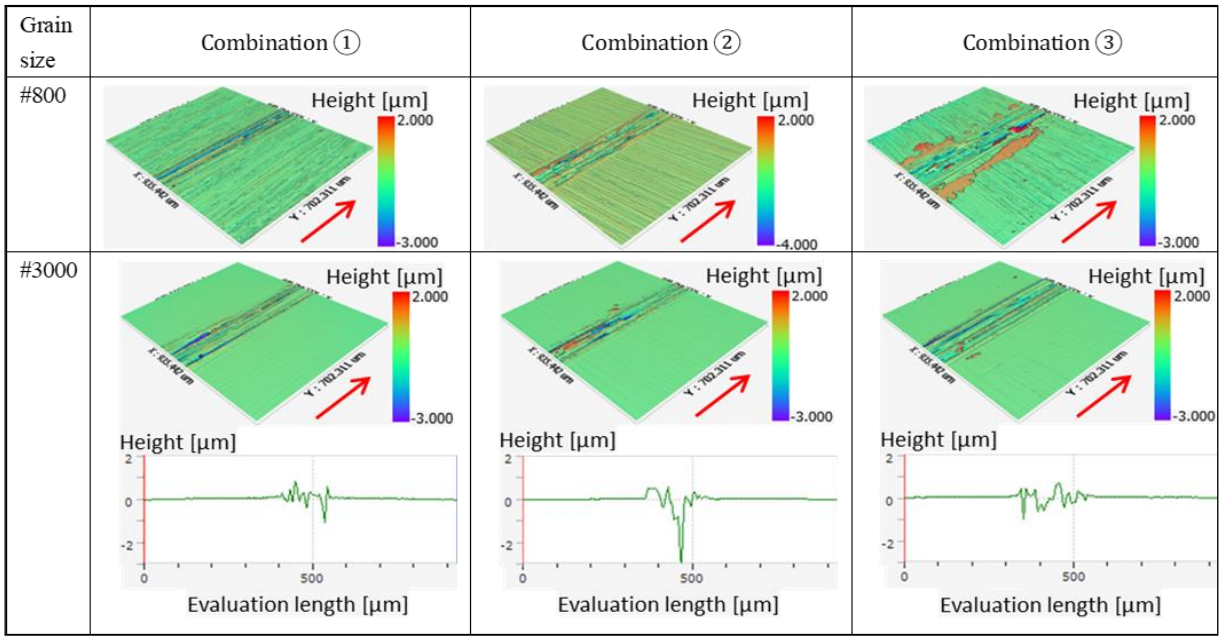

Fig. 10. Typical images of each block surface after friction tests. Arrows denote sliding direction.

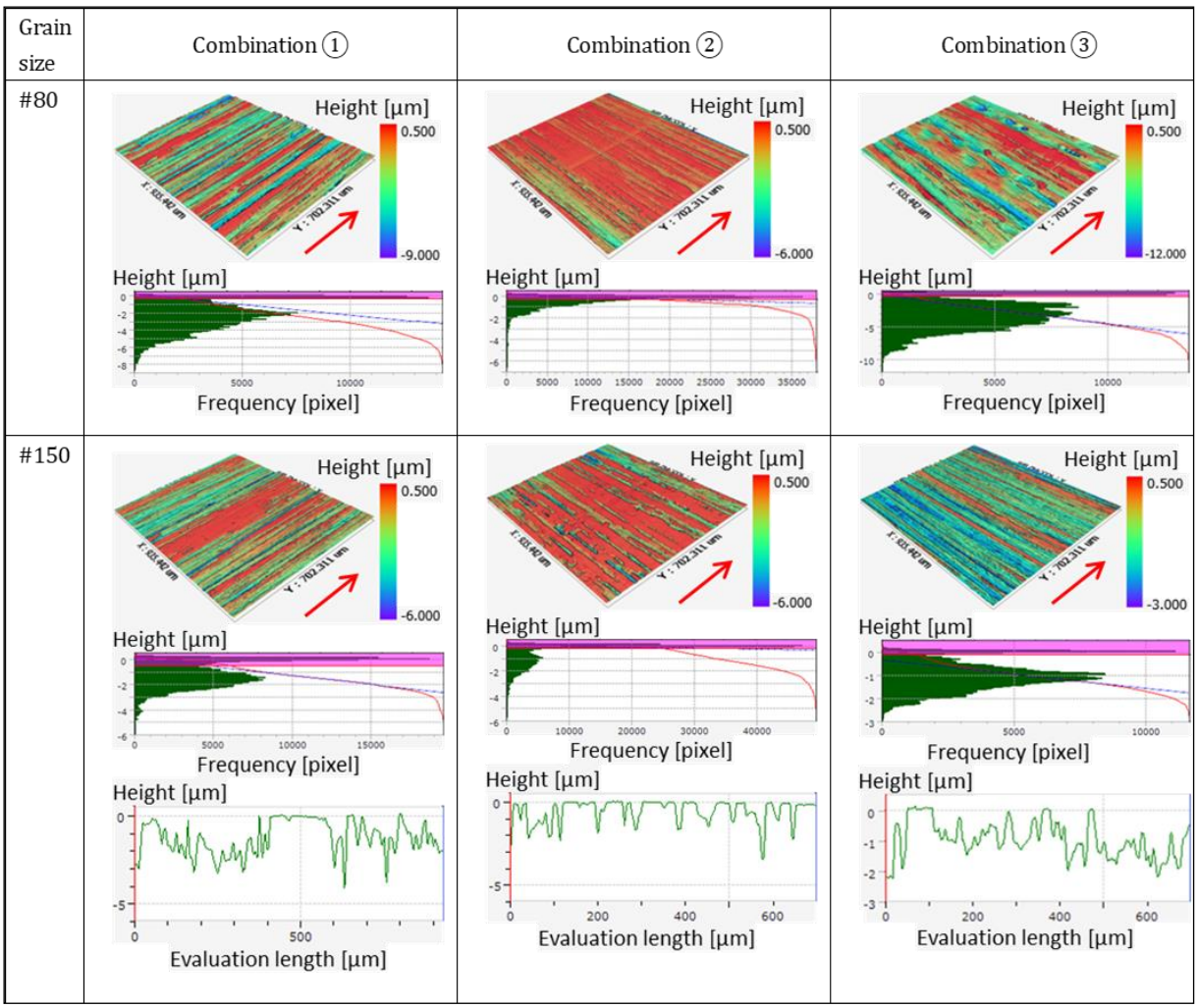

Fig. 11. Typical images of each block surface after friction tests. Arrows denote sliding direction.

Additionally, it is likely that the wear powder generated could not escape to the valleys (recesses) on the rough surfaces, which resulted in abrasive wear caused by wear powder under all anisotropic combination conditions.

In contrast, Fig. 11 presents example surface images and height histograms of test pieces #80 and #150, and a cross-section profile test piece #150 polished test piece, captured after the friction tests. One can see that compared to the initial surface presented in Fig. 3, the surface that originally had peaks became planar, indicating that the wear resulted from solid materials coming into contact.

The type of contact and area of wear differed significantly depending on the anisotropic combination conditions. The wear area decreased in size in the order of condition ② > condition ① > condition ③. This order matches the relative order of friction coefficients presented in Fig. 9. Three broad friction factors caused by solid materials coming into contact are the resistance to overcome the unevenness of the surfaces, digging resistance, and shear resistance of the adhesion area [10]. In particular, resistance caused by adhesion is known to be the major determining factor of frictional force. Furthermore, because the frictional force caused by adhesion is proportional to the true contact area of adhesion and positively correlated to the contact and wear areas, as well as the friction coefficient, it is presumed that for test pieces #80 and #150, the change in friction coefficient was largely affected by adhesion and wear.

The effects of different wear areas based on the anisotropic combination conditions for test pieces #80 and #150 are discussed below. Under anisotropic combination condition ②, the crease directions of the surface roughness on the block and the plate were parallel and the sliding

direction was orthogonal to the crease direction. It is assumed that the peaks of the surface roughness were mutually sheared, causing intermittent contact, which resulted in faster wear and a relatively large friction coefficient of 0.45 based on the large wear area.

In contrast, under anisotropic combination condition ①, the crease directions of the surface roughness on the block and the plate, as well as the sliding direction, were all parallel. It is assumed that under these contact conditions, the peaks of the surface roughness were in contact along the crease lines. As a result, while there was friction between the peaks, because total surface contact did not occur, these conditions resulted in a friction coefficient of approximately 0.3.

Under anisotropic combination condition ③, the crease directions of the surface roughness on the block and the plate were orthogonal, meaning the contact area was limited to an extent because the peaks of the surface roughness were only in contact at certain points. It is assumed that this resulted in lower wear and a corresponding low friction coefficient of 0.15.

The relationship between wear and the friction coefficient of the surfaces of test pieces #80 and #150 was investigated in greater detail based on the above results.

In in Fig. 11, the red area of the surface image, as well as the semi-transparent area of the height histogram, represent the planar area formed as a result of the friction tests. This area experienced wear based on the contact between solid materials. Accordingly, by considering the semi-transparent area in the height histogram to be the area of contact and wear between the solid materials, the proportion of this area over the total area of measurement was defined as the wear area ratio and the relationship between this ratio and the average friction coefficient was estimated.

The results obtained are presented in Fig. 12. These results confirm the definite trend that the friction coefficient increases as the wear area ratio (i.e., contact area) increases. Accordingly, it can be argued that in cases of test pieces #80 and #150, the differences in contact conditions caused by different anisotropic combination conditions resulted in the differences in wear conditions. Additionally, the differences in the friction coefficients resulted from differences in the contact areas.

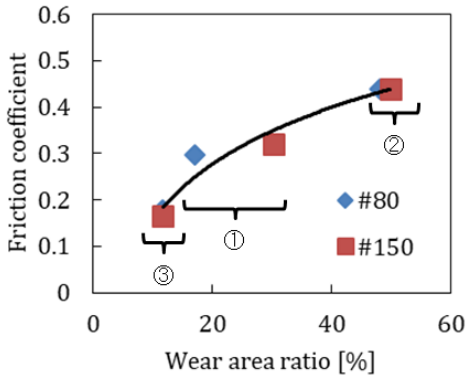

Fig. 12. Relationship between wear area ratio and average friction coefficient.

Based on the aforementioned results of the investigations of the initial surface morphologies of the solid materials to obtain a basic understanding of the sliding phenomenon between contacting solid materials, we found that the lowest friction coefficients were achieved for test pieces #80 and #150 under anisotropic combination condition ③. This means that when considering severe sliding conditions, imparting surface roughness equivalent to the polishing of test piece #80 or #150 and arranging the anisotropic combination conditions such that the crease directions are orthogonal to each other and the crease direction of the moving body and sliding direction are parallel can be considered as an optimal configuration.

4. CONCLUSIONS

The major findings from our systematic investigation of solid frictional characteristics under anisotropic combination conditions and the surface roughness of materials, which was conducted to acquire a basic understanding of the phenomena of contact and sliding between solid materials, are summarized below:

1) For test pieces #800 and #3000, the friction coefficient did not change based on the anisotropic combination conditions. Our tests revealed a friction coefficient of approximately 0.35.

2) For test pieces #80 and #150, the friction coefficient changed significantly depending on the anisotropic combination conditions.

Our tests revealed a friction coefficient of approximately 0.45 under the anisotropic combination condition where the crease directions were parallel and the sliding direction was orthogonal to the crease direction, friction coefficient of approximately 0.3 under the anisotropic combination condition where the crease directions were parallel and the sliding direction was parallel to the crease direction, and friction coefficient of approximately 0.15 under the anisotropic combination condition where the crease directions were orthogonal and the sliding direction was parallel to the crease direction of the moving body.

3) When considering an initial surface roughness that can be adopted under severe sliding conditions involving contact between solid materials, an initial surface roughness equivalent to that of test piece #80 or #150 under anisotropic combination conditions where the crease directions of the solid materials are orthogonal and the sliding direction is parallel to the crease direction of the moving body is optima.

It should be noted that because the friction tests were performed utilizing solid materials with random and irregular surfaces based on polishing utilizing emery paper, although the results obtained may be utilized as a guideline for surface design, it is difficult to adopt them as quantitative design criteria. In the future, it will be necessary to study frictional characteristics by conducting friction tests to facilitate quantitative surface texture design by preparing and utilizing test pieces with reproducible artificially processed surface textures.

Acknowledgement

The authors express their gratitude to Associate Professor Takeichi Yoshinori of the Toyohashi University of Technology for his advice and help in conducting this study.

REFERENCES

[1] K. Holmberg, P. Andersson, A. Erdmir, *Global energy consumption due to friction in passenger cars*, Tribology International, vol. 47, pp. 221-234, 2012, doi:10.1016/j.triboint.2011.11.022

[2] T. Nakamura, *Improvement of fuel efficiency of passenger cars by taking advantage of tribology*, Tribology Online, vol. 12, no. 3, pp. 76-81, 2017, doi:10.2474/trol.12.76

[3] C. Gachot, A. Rosenkranz, S.M. Hsu, H.L. Costa, *A critical assessment of surface texturing for friction and wear improvement*, Wear, vol. 372-373, pp. 21-41, 2017, doi:10.1016/j.wear.2016.11.020

[4] B. Ivkovic, M. Đurdanovic, D. Stamenkovic, *The Influence of the Contact Surface Roughness on the Static Friction Coefficient*, Tribology in Industry, vol. 22, no. 3&4, pp. 41-44, 2000.

[5] M. Sedlaček, B. Podgornik, J. Vižintin, *Influence of surface preparation on roughness parameters, friction and wear*, Wear, vol. 266, iss. 3-4, pp. 482-487, 2009, doi:10.1016/j.wear.2008.04.017

[6] M. Sedlaček, B. Podgornik, J. Vižintin, *Correlation between standard roughness parameters skewness and kurtosisand tribological behaviour of contact surfaces*, Tribology International, vol. 48, pp. 102-112, 2012, doi:10.1016/j.triboint.2011.11.008

[7] Y. Miyakawa, *Surface roughness and friction*, Journal of the Society of Mechanical Engineers, vol. 58, pp. 79-84, 1955.

[8] P.L. Menezes, Kishore, S.V. Kailas, *Influence of surface texture and roughness parameters on friction and transfer layer formation during sliding of aluminium pin on steel plate*, Wear, vol. 267, iss. 9-10, pp. 1534-1549, 2009, doi:10.1016/j.wear.2009.06.003

[9] P.L. Menezes, Kishore, S.V. Kailas, M.R. Lovell, *Influence of Surface Texture and Roughness of Softer and Harder Counter Materials on Friction During Sliding*, Journal of Materials Engineering and Performance, vol. 24, iss. 1, pp. 393-403, 2015, doi: 10.1007/s11665-014-1304-1

[10] T. Tukizoe, *Surface roughness and friction*, Journal of Japan Society of Lubrication Engineers, vol. 19, no. 2, pp. 91-98, 1974.